Available online at www.sciencedirect.com
SCIENCE DIRECT®
C. R. Physique 5 (2004) 453–461
COMPTES RENDUS PHYSIQUE

Ultimate energy particles in the Universe/Particules d'énergies ultimes dans l'Univers

Propagation of ultra high energy cosmic rays

Todor Stanev

Bartol Research Institute, University of Delaware Newark, Delaware Newark, DE 19716, USA

Available online 24 April 2004

Presented by Pierre Encrenaz

Abstract

All particles of energy approaching 10^{20} eV interact inelastically in the microwave background and other astrophysical photon fields and lose energy. We describe briefly the energy loss processes and show the consequences of proton propagation in extragalactic space. We also discuss the influence of astrophysical magnetic fields on the propagation. ***To cite this article: T. Stanev, C. R. Physique 5 (2004).***

Résumé

Propagation des rayons cosmiques ultra-énergétiques. Tout rayon cosmique dont l'énergie est proche de 10^{20} eV subit des interactions inélastiques avec le fond cosmologique micro-onde ou avec d'autres champs de photons d'origine astrophysique, en perdant une partie de son énergie. Nous décrivons brièvement les mécanismes de perte d'énergie et en analysons les conséquences sur la propagation de protons dans l'epace extra-galactique. Nous décrivons également l'effet des champs magnétiques d'origine astrophysique sur la propagation. ***Pour citer cet article : T. Stanev, C. R. Physique 5 (2004).***

Keywords: Microwave background; Energy loss; GZK cutoff; Magnetic fields (galactic and extragalactic)

Mots-clés : Rayonnement fossile ; Perte d'énergie ; Coupure GZK ; Champs magnétiques (galactiques et extra-galactiques)

1. Introduction

Most of the theoretical interest in the highest energy cosmic rays during recent years has been aimed at the explanation of the production mechanisms for these events. The other puzzling side of the phenomenon is how these ultra high energy particles can penetrate from their sources to us through the dense photon fields of the Universe. All stable ultra high energy particles, except for neutrinos, lose energy in such interactions. If the detected events are of extragalactic origin, the details of these energy losses shape their energy spectrum as much as their production mechanisms do.

In 1963 John Linsley [1] reported the detection of an air shower of energy exceeding 10^{20} eV. This was an important, but not surprising, result because at the time the physicists assumed that the cosmic ray spectrum may continue to infinitely high energy. The cosmic microwave background (CMB) radiation was discovered three years later and immediately after that two papers that predicted the end of the cosmic ray spectrum appeared [2,3] almost simultaneously. These papers calculated the interaction cross section of protons of energy 10^{20} eV with the newly discovered radiation and concluded that their sources should not be further away than one hundred megaparsecs (1 Mpc $= 3 \times 10^{24}$ cm).

The back of the envelope estimate goes like this: the average interaction length $\lambda_{\rm ph}$ for proton photoproduction interactions with the microwave background is the inverse of the product of the interaction cross section $\sigma_{\rm ph}$ and the photon density n. For $\sigma_{\rm ph} = 10^{-28}$ cm^2 and $n = 400$ cm^{-3}, $\lambda_{\rm ph} = 8.3$ Mpc. Since protons lose about 0.2 of their energy in each interaction it takes about ten interaction lengths to decrease the particle energy by a factor of 10.

E-mail address: stanev@bartol.udel.edu (T. Stanev).

1631-0705/$ – see front matter
doi:10.1016/j.crhy.2004.03.014

This conclusion is now universally accepted and the distance to the sources of the ultra high energy cosmic rays is restricted even more. In the contemporary cosmic ray propagation research the main interest is in the strength and level of organization of the extragalactic magnetic fields. The magnetic fields are important because they scatter protons and thus increase the proton pathlength from a source at given luminosity distance. Magnetic fields are even more important for the propagation of high energy γ-rays. Gamma rays create e^+e^- pairs in interactions with ambient photon fields. In the presence of magnetic fields electrons lose energy on synchrotron radiation very fast.

There is no consensus, however, about the strength of the extragalactic magnetic fields and the existence of ordered extragalactic fields. Scientists who believe in relatively strong fields point at the μgauss fields that are observed in clusters of galaxies. The opposite argument is that primordial magnetic fields are very low – not higher than 10^{-17} G and the Universe is too young to amplify these low fields by a factors of 10^7–10^8.

2. Proton energy loss

There are two ways in which protons interact on the ambient photon fields: photoproduction and e^+e^- pair production. At least one pion is generated in the first process. This requires that the center of mass energy of the interaction $\sqrt{s}$ is higher that the sum of a proton mass m_p and a pion mass m_π. In the laboratory system the square of the center of mass energy s is

$$s = m_p^2 + 2E_p\varepsilon(1-\cos\theta), \tag{1}$$

where ε is the photon energy and θ is the angle between the proton and the photon. In a head on collision ($\cos\theta = -1$) with a photon of the average CMB energy (6.3×10^{-4} eV) the minimum proton energy is

$$E_p = \frac{m_\pi}{4\varepsilon}(2m_p + m_\pi) \simeq 10^{20}\ \text{eV}. \tag{2}$$

There are many CMB photons with higher energy and the threshold proton energy is actually lower.

The cross section for this interaction is very well studied at accelerators where photons interact with stationary protons. The highest cross section is at the mass of the Δ^+ resonance (1232 MeV) which decays to either a proton and a neutral pion ($p\pi^0$) or to a neutron and a positive pion ($n\pi^+$). At the peak of the resonance the cross section is about 500 μb. At higher energy the cross section first decreases to about 100 μb and then increases logarithmically. The neutron interaction cross section is, if not identical, very similar to the proton one.

The CMB spectrum and density are also very well known, so the proton interaction length can be calculated exactly, as shown in the left-hand panel of Fig. 1 with dash line. Since protons lose only a fraction of their energy (K_{inel}), another quantity – the energy loss length $L_{\text{loss}} = -\frac{1}{E}\frac{\mathrm{d}E}{\mathrm{d}x}$ becomes important. The energy loss length is longer than the interaction length by $1/K_{\text{inel}}$, by about a factor of 5 at threshold. At higher energy K_{inel} grows and this factor is about 2.

The other process is the electromagnetic production of e^+e^- pairs, identical to the photon interactions in the nuclear electromagnetic field. The addition of two electron masses to the center of mass energy $\sqrt{s}$ requires much lower proton energy

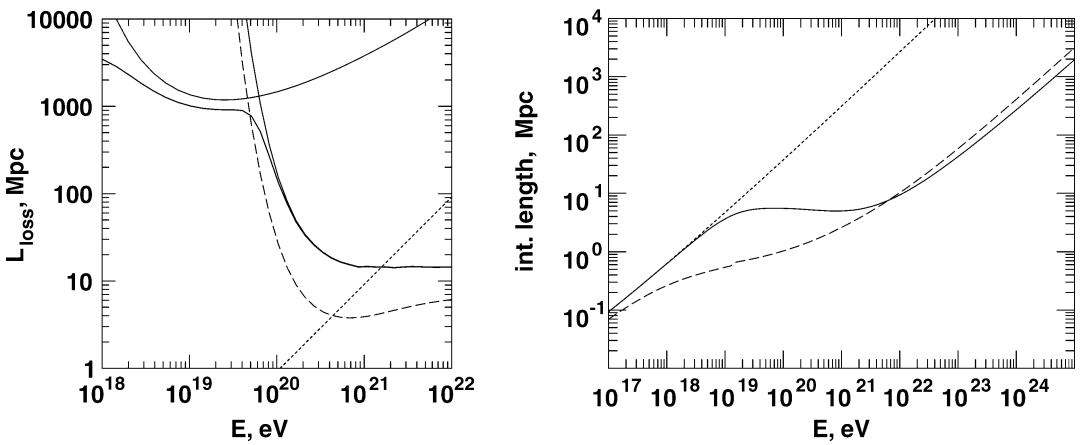

Fig. 1. Left-hand panel: proton energy loss. The dashed line shows the proton interaction length for photoproduction on the microwave radiation. The thin solid lines are the energy loss distances for photoproduction and pair production and the thick solid line is their sum. The dotted line is the neutron decay length. Right-hand panel: γ-ray and electron interaction lengths. The dotted line is the γ-ray interaction length in the absence of radio background.

and the process has lower threshold. The cross section for pair production is higher than $\sigma_{\rm ph}$, but the fractional energy loss is small, of order of the ratio of the electron to proton mass m_e/m_p. The energy loss length has a minimum around 2×10^{19} eV and is always longer than 1000 Mpc.

The last proton energy loss process is the redshift due to the expansion of the Universe. The current energy loss length to redshift is the ratio of the velocity of light to the Hubble constant (c/H_0) and is 4000 Mpc for $H_0 = 75$ km s^{-1} Mpc^{-1}.

The dotted line in the left-hand panel of Fig. 1 shows the decay length of neutrons. It intersects the proton interaction length at energy about 4×10^{20}. Neutrons of lower energy will then most likely decay and only neutrons of higher energy are likely to have photoproduction interactions.

3. Gamma ray energy loss

Gamma rays also lose energy in interactions in photon backgrounds. The main process is the production of electron–positron pairs $\gamma\gamma \to e^+e^-$. The process has a resonant character and the cross section peaks at $E_\gamma \varepsilon = m_e^2$, where ε is the energy of the seed photons. For the average energy of CMB this corresponds to E_γ of 8×10^{14} eV and the mean free path increases with increasing E_γ. For gamma rays of energy 10^{20} eV the relevant seed photon frequency is about 1 MHz – in the radio band. This creates a big uncertainty in the estimates of the UHE γ-ray energy loss because the density of the radio background at such frequencies is not known. One can relate the radio emission of various astrophysical objects to the much better known infrared emission and generate models. In the right-hand side panel of Fig. 1 the interaction length $\lambda_{\gamma\gamma}$ is shown with solid line for one such model [4] of the radio background. The dotted line shows $\lambda_{\gamma\gamma}$ for interactions only on the CMB. Independently of the existence of the radio background the gamma ray propagation is restricted to about 120 Mpc by the creation of two pairs ($\gamma\gamma \to e^+e^-e^+e^-$) on the CMB.

The next step in the γ-ray propagation depends very strongly on the strength of the extragalactic magnetic fields. If they are negligible the electrons have inverse Compton interactions, whose interaction length is shown with dashed line, and generate a second generation of very high energy γ-rays. This cascading can continue for a significant distance without downgrading very much the gamma ray energy. If, however, the magnetic fields are significant electrons lose energy very fast on synchrotron radiation. The γ-ray energy is rapidly transferred to the MeV-GeV energy range. The range of top–down cosmic ray generation models has been restricted because of overproduction of GeV γ-rays. The energy loss distance on synchrotron radiation is $2.6 E_{18}^{-1} B_{-9}^{-2}$ Mpc, where E_{18} is the electron energy in unites of 10^{18} eV and B_{-9} is the strength of magnetic field in ngauss.

Finally, γ-rays of energy above 10^{20} eV interact with the geomagnetic field and produce e^+e^- pairs when they approach the Earth. Subsequent electromagnetic cascading transfers the energy of the primary γ-ray to a group of lower energy particles. The exact threshold for the process depends on the angle between the γ-ray trajectory and the geomagnetic field lines.

4. Energy loss of heavy nuclei

Nuclei heavier than protons are photodisintegrated [5] in interactions with the microwave background. The main process is the giant dipole resonance which requires the deposit of energy 10–20 MeV in the nuclear frame. Heavy nuclei lose one nucleon at a time but the cross section is high. Protons are lost easier than neutrons, the nucleus is destabilized and the decay of the unstable fragments contributes to the disintegration. The process depends of the nucleus Lorentz factor – on its energy per nucleon. He nuclei are disintegrated at the lowest total energy per nucleon – slightly above 10^{20} eV the energy loss distance for He is about 8 Mpc. Iron nuclei reach the minimum energy loss distance only above 10^{21} eV, but it is only about 1 Mpc.

5. Propagation of protons: production of secondary signals

The experimental hints that at least a large fraction of UHECR are protons and the very well-known proton energy losses encourage exact calculations of proton propagation. The problem has been studied by different means – solutions of transport equations [6], Monte Carlo codes [7–10] and intermediate numerical approaches [11]. Solutions of the transport equations permit the derivation of the general features of the proton energy spectrum after propagation. The Monte Carlo approach has the advantage of the application of the exact form of the proton energy loss and study of the fluctuations in the proton energy loss. This is important, as first realized by Hill and Schramm [7] because the energy loss in photoproduction interactions has stochastic character and cannot be modeled exactly as continuous energy loss.

Fig. 2 demonstrates the effect of the propagation in the microwave background of protons of different energy. The left-hand panel of the figure shows the energy distribution of protons injected with energy between $10^{21.0}$ and $10^{21.2}$ eV after propagation

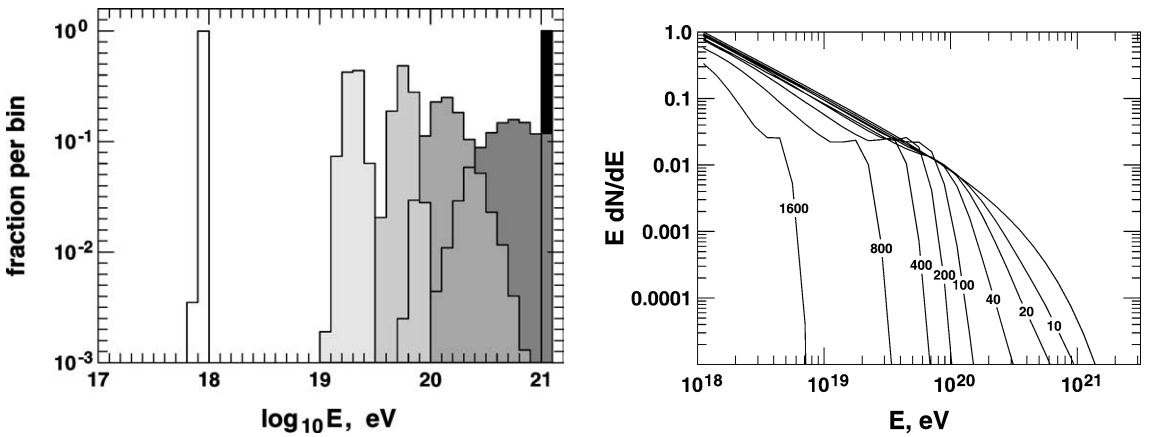

Fig. 2. Left-hand panel: propagation of protons injected with energy between $10^{21.0}$ and $10^{21.1}$ eV on distances of (from right to left, decreasing shading) 10, 40, 200, 800 and 3200 Mpc. Right-hand panel: evolution of the cosmic ray injection spectrum (smooth curve) after propagation on different distances. The propagated spectra are scaled with $\mathrm{d}t/\mathrm{d}z$. The distances are indicated by the appropriate curves.

on distances of 10, 40, 200, 800 and 3200 Mpc. After propagation on 10 Mpc slightly more than 10% of the injected protons retain their injection energy. The energy distribution is very wide, covering one order of magnitude. The distribution is still wide after 40 Mpc, although none of the 10 000 injected protons retains its injection energy. At larger distances the distribution becomes narrower. The reason is that higher energy particles still lose energy in photoproduction interactions while lower energy ones have smaller energy loss on e^+e^- pair production and redshift. With increasing propagation distance the proton energy distribution is almost as narrow as at injection and the average energy is lower by three orders of magnitude.

The right-hand panel of Fig. 2 presents the evolution of cosmic ray spectrum injected with energy distribution $N(E) = E^{-2}\exp(-E/E_{\max})$ ($E_{\max} = 10^{21.5}$) after propagation at different distances. Each proton energy distribution is scaled with the duration of the injection Δt, which decreases with the redshift. At distances less than 20 Mpc the spectrum is only depleted in its highest energy particles. At about 40 Mpc, however, the protons that have had significant energy loss start to accumulate and form a feature just below 10^{20} eV where the photoproduction mean free path grows fast. With increasing distance the feature moves to smaller energy and becomes more prominent. At still larger distances, above 400 Mpc, one sees a prominent dip at energy below 3×10^{19} eV which is due to the e^+e^- production energy loss. These main features of the cosmic ray propagation were first described by Berezinsky and Grigorieva [6].

At distances exceeding 1000 Mpc the spectrum is contracted on its high energy side and practically does not contribute to the flux of the high energy cosmic rays. The reason it does not contribute much to the 10^{18} eV cosmic rays is that the duration of injection Δt is significantly smaller than at current time.

One can use the right-hand panel of Fig. 2 to limit the distance to the cosmic ray sources that contribute to different energy ranges of the detected UHECR. Even with $E_{\max}$ as high as assumed above only sources closer than 100 Mpc can be responsible for the majority of cosmic rays above 10^{20} eV. The cut-off distance for particles above 10^{19} eV exceeds one Gpc.

Except the energy loss due to redshift, all other energy losses should be transfered to particles generated in the proton interactions in the microwave background. In the astrophysical environment all unstable secondary particles decay and only the stable γ-rays and neutrinos appear as final products of the interactions. The ratio between γ-rays and neutrinos depends on the interaction energy. The Δ^+ resonance creates twice as many γ-rays through the $\pi^0 \to \gamma\gamma$ channel as it generates neutrinos in the $\pi^+ \to \mu^+\nu_\mu \to e^+ + \nu_e + \nu_\mu + \bar{\nu}_\mu$ channel. At higher center of mass energy the ratio is reversed as two times more charged pions are generated than neutral ones. Neutrinos traverse the Universe freely while γ-rays and electrons lose energy in pair production, inverse Compton effect and synchrotron radiation as described above. Energy losses on pair production contribute only to the electromagnetic secondaries. The fate of these, and all other, electrons depends mostly on the strength of the magnetic fields at the location of the interactions.

Whatever these fields are every source of UHECR should be surrounded by a halo of γ-rays and neutrinos. If there are no considerable magnetic fields, the electromagnetic energy lost by the protons will be slowly transferred to lower energy γ-rays and electrons and this electromagnetic cascade will not be observable. For high magnetic fields the electron component would quickly transfer its energy to TeV γ-rays that could eventually be detected.

The flux of secondary neutrinos from cosmic ray proton propagation (cosmogenic neutrinos) depends on the parameters of the accelerated protons and on the distribution of the UHECR sources in the Universe that are briefly discussed in the next section. We only know that these are very high energy neutrinos whose flux peaks at energies of 10^{17}–10^{18} eV because only

the highest energy protons have photoproduction interactions. In case of isotropic homogeneous cosmic ray source distribution the cosmogenic neutrinos will form an isotropic neutrino background.

6. Formation of the proton energy spectrum after propagation

Predictions of the shape of the cosmic ray spectrum, assuming that it consists of protons, requires much more than the proton energy loss in propagation. The necessary astrophysical input, currently unknown, includes et least the following four items:

- UHECR source distribution;
- cosmic ray source luminosity;
- cosmic ray injection (acceleration) spectrum;
- cosmic ray source cosmological evolution.

The UHECR source distribution is the least known one. We expect the input to come from future observational results. The current experimental statistics does not allow any conclusions, except the existence of some cosmologically close by sources responsible for the observed events above the GZK cut-off.

The other three parameters are not independent of each other. The UHECR source luminosity can in principle be determined by the detected UHECR flux above 10^{19} eV. In view of the low current statistics, the derived luminosity depends strongly on the assumed injection spectrum and partially on the assumed cosmological evolution of the sources. The source cosmological evolution may be the best known parameter since it should resemble these of other astrophysical phenomena such as the star formation rate in the Universe.

A natural assumption for the source distribution is that sources are isotropically and homogeneously distributed in the Universe because we do not inhabit a special part of it. In such a case the cosmic ray flux at Earth could be determined by an integration of the fluxes shown in the right-hand panel Fig. 2 for various assumptions for the cosmic ray luminosity, injection spectrum and cosmological evolution of the sources, i.e.,

$$N(E) = \int_0^{z_{\max}} \int_E^{E_0} L(z) N_0(E_0) P(E_0, E', z) \frac{\mathrm{d}t}{\mathrm{d}z} \mathrm{d}E' \, \mathrm{d}z, \tag{3}$$

where $L(z)$ is the cosmic ray source luminosity as a function of redshift and $N_0(E_0)$ reflects the injection spectrum, $P(E_0, E', z)$ is the probability for a proton injected with energy E_0 at redshift z to reach us with energy E'. The derivative $\mathrm{d}t/\mathrm{d}z$ depends on the cosmological model and is $(1+z)^{-5/2}$ for the Einstein–deSitter Universe.

Fig. 3 shows spectra obtained after a numerical integration of propagation calculations as shown in Fig. 3 multiplied by E^3 as the experimental results are usually presented. The left-hand panel corresponds to five different injection spectra, all with an exponential cut-off at $10^{21.5}$ eV and two assumptions for the cosmological evolution of the UHECR sources. Note that the

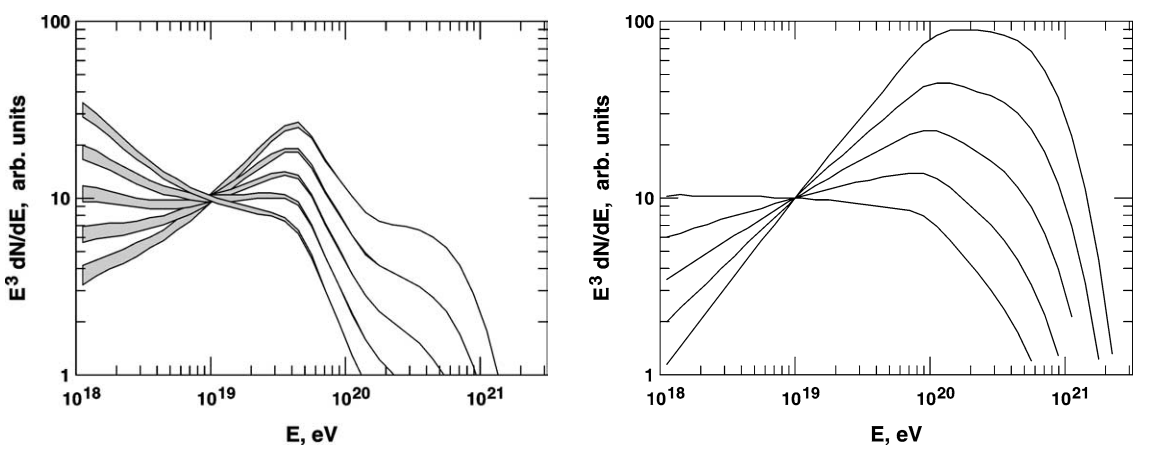

Fig. 3. Left-hand panel: spectra at Earth for isotropic homogeneous source distribution of the cosmic ray sources and power law injection spectra with indices 2.0, 2.25, 2.50, 2.75, and 3.0. The upper edge of the shaded bands is for source cosmological evolution $(1+z)^4$ and the lower edge for $(1+z)^3$. Right-hand panel: same spectra if all UHECR come from a source at a distance of 20 Mpc.

cosmological evolution of the sources generates only a small difference between the spectra, and only below 10^{20} eV because the highest energy part of the spectrum is generated by cosmologically nearby sources. Without any fits one may conclude that injection spectra close to $E_0^{-2.5}$ fit better the experimental spectra above $10^{18.5}$ eV, which have a power law index close to E^{-3}.

The right-hand panel of Fig. 3 shows the arrival energy distribution if all cosmic rays come from a single source at distance 20 Mpc. The shapes of the energy spectra in this assumption match the experimental data much worse.

A comparison between the two panels of Fig. 3 shows that a much better measurement of the exact shape of the cosmic ray spectrum could bring information about the source distribution, or at least restrict some of the models for their origin.

7. Propagation in magnetic fields

The figures shown in the previous section are generated without taking into account the possible existence of extragalactic magnetic fields. As far as proton propagation is concerned, magnetic fields introduce three main effects. The proton scattering increases the propagation pathlength and thus restricts the radius of the possible sources even more. The scattering creates a deviation of the arrival direction of the UHE protons from the direction of the source. The gyro radius of a 10^{20} eV proton in 10^{-9} G (nG) field is 100 Mpc. If the field is random with a correlation length ℓ the deviation angle $\langle\theta\rangle$ after propagation on distance D is

$$\langle\theta\rangle \simeq 2.53^\circ B_{-9} D_{100}^{1/2} \ell_1^{1/2} E_{20}^{-1}, \tag{4}$$

where B_{-9} is the r.m.s. field strength in nG, D_{100} is the distance in units of 100 Mpc, ℓ_1 is the correlation length in units of 1 Mpc and E_{20} is the energy in units of 10^{20} eV. Protons below 10^{20} eV would scatter much more around the direction of the source but the highest energy particles would point at the source with an angle comparable to the experimental resolution.

The scattering also introduces time delay compared to the rectilinear propagation of light. The time delay $\delta\tau$ depends much stronger on the particle energy, magnetic field strength and the propagation distance. For small angle scattering it is

$$\delta\tau \simeq 3 \times 10^5 B_{-9}^2 D_{100}^2 \ell_1 E_{20}^{-2} \text{ years}. \tag{5}$$

If the source of the observed UHECR were an explosive process, such as a gamma ray burst at a distance of 100 Mpc, all protons would be accelerated at once, but because of time delay they would arrive at Earth in a reverse order of their energy. The highest energy particles would reach us first, while the lower energy ones would be delayed with millions of years. It is important to note that the time delay depends on the square of the particle charge. Iron nuclei coming from 10 Mpc will be still delayed seven times more than protons arriving from 100 Mpc.

Time delays could prevent some of the extragalactic protons from reaching us, because their travel time could exceed the the age of the Universe. Particles of energy below 5.5×10^{17} eV from the gamma ray burst at 100 Mpc, for example, will not reach us because their time delay will exceed Hubble time, taken here of 10^{10} years for simplicity.

Fig. 4 (left-hand panel) shows with a thick gray line the restriction of the distance to the UHE proton sources as a function of the particle energy according to Eq. (5). This equation, however, may not calculate properly the time delay at 'low' energy because of the small angle scattering assumption used in its derivation. The solid and open circles show the proton horizon R_{50},

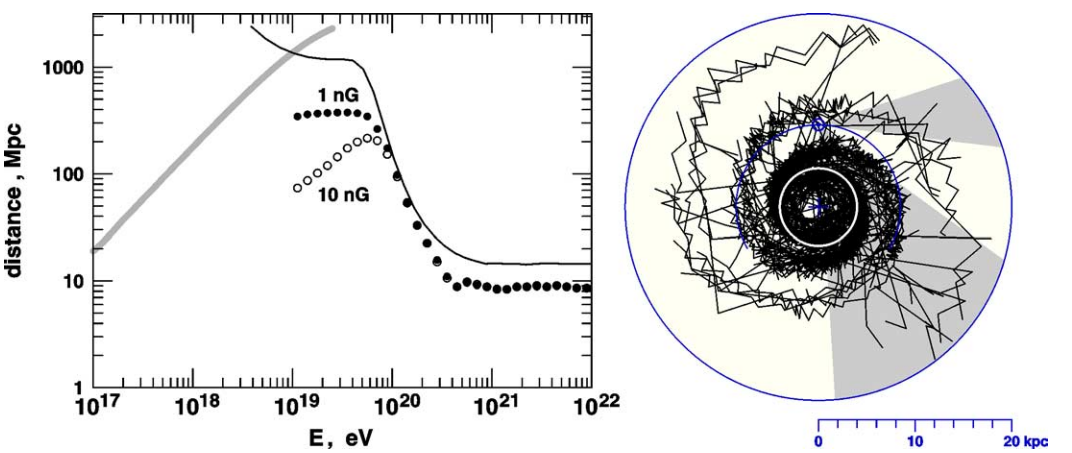

Fig. 4. Left-hand panel: cosmic ray protons horizon as a function of the proton energy: see text. Right-hand panel: propagation of 10^{18} eV protons in the Galactic magnetic field.

as derived in [10] for random fields of strength 1 nG and 10 nG respectively. R_{50} is the distance at which $1/e$ fraction of protons maintain at least one half of their injection energy. The solid line shows the proton energy loss distance.

The account for the magnetic field restricts the source distance even at the highest energy. It is always below 10 Mpc and the magnetic field strength is not very important. The difference appears below 10^{20} eV, where the horizon stays constant at about 300 Mpc – a factor of 4 below the energy loss length for field strength of 1 nG. For field of 10 nG the trend reverses and the horizon for lower energy particles decreases. to less than 100 Mpc at 10^{19} eV. Since Eq. (5) does not include any energy loss, it gives the maximum distance allowed for protons in the 10^{18}–10^{19} eV range.

7.1. Galactic magnetic fields

The magnetic field of our Galaxy is a good example for a combination of organized and random magnetic fields, which most likely exist on different scales in the Universe. The regular field $B_{\rm reg}$ in the Galaxy has a spiral structure of axisymmetric or bisymmetric type resembling the matter distribution. The local strength of the field is about 1.8 μG with direction pointing inwards approximately along the Orion arm. The strength of the random field is not known exactly, with estimates between $1/2$ and 2 $B_{\rm reg}$. The correlation length ℓ of the random galactic fields is of order 50 to 100 pc. More general estimates of the total field strength over the whole Galaxy give 5–6 μG, and it is possible that a Galactic halo field, that does not contribute much locally, also exists. It is likely that the random field dominates the total field strength within the Galactic arms, while the regular field is dominant in the interarm space.

The right-hand panel of Fig. 4 shows an example for propagation of 10^{18} eV protons emitted isotropically at the 4 Kpc circle (indicated in white) in a galactic field model. The position of the Solar system is also indicated with $\odot$. The figure plots the points where the protons cross the galactic plane. Most of the protons are trapped by the regular field and gyrate around the magnetic field lines. Since there is a random component, protons are occasionally deflected by it and may be trapped by another of the magnetic spirals. The two shaded areas correspond to directions in which the AGASA experiment observes an excess [12] of comic rays of that energy. This example is also valid for the propagation of heavy nuclei of total energy $Z \times 10^{18}$ eV in the Galaxy. Models of UHECR acceleration in the Galaxy tend to produce iron nuclei. Since the regular Galactic field is known much better than in order of magnitude, a precise measurement of the cosmic ray anisotropy in the 10^{19}–10^{20} eV energy range could answer the question if UHECR are heavy nuclei accelerated in the Galaxy inside the solar circle, or they are of extragalactic origin.

This example gives us an idea how an organized field influences the cosmic ray propagation. The random walk scattering initiated by random fields is replaced by motion driven by the field geometry. At higher energy the proton trajectories are almost straight lines and the deflection in the Galactic field for 10^{20} eV protons is between 2° and 5° depending on the exact magnetic field model and on the initial direction of the proton. Field models with alternating polarity give the smallest deflections, while models with a z component of the field (perpendicular to the galactic plane) cause the largest ones.

7.2. Ordered extragalactic fields

The possible existence of regular large scale fields makes the consequences of proton propagation even more complicated. The following exercise in [13] demonstrates the problems in the following geometry: a cosmic ray source at the origin injects isotropically protons above $10^{18.5}$ eV on a power law spectrum with spectral index of 2 and exponential cutoff at $10^{21.5}$ eV. The source is in the central yz plane of a 3 Mpc wide magnetic wall, that is a simplified version of the Supergalactic plane [14] (SGP), which is the plane of weight of galaxies within redshift of 0.05. Magnetic field with strength of $B_{\rm reg} = 10$ nG fills the SGP, points in z direction and decays exponentially outside the SGP. The regular field is accompanied by random field with strength $B_{\rm rndm} = B_{\rm reg}/2$.

Protons are followed with energy loss until they intersect a sphere of radius 20 Mpc. Their exit positions, velocity vectors and energies are recorded. The correlation between these parameters are studied with this simulation. Fig. 5 shows the energy spectrum of protons leaving the sphere at two 9 Mpc^2 patches: the *front* patch around $z = 20$ Mpc inside the SGP, and the *side* patch with the same area around $x = 20$ Mpc, i.e., in direction perpendicular to the magnetic field.

The locations of the two patches in Fig. 5 are chosen because the exit proton spectra are very different at these positions. Protons of energy below 10^{20} eV are often caught in the SGP magnetic field and cannot leave it. They gyrate back and forth around the magnetic field lines and are equally likely to leave the 20 Mpc sphere through the *front* and the symmetric *back* patches. Because of these particles that are trapped in the magnetic wall the exit spectra at 10^{19} eV in these patches are higher than the injection spectra by 2 orders of magnitude. At higher energies the protons propagate almost rectilinearly. The decrease at high energy is due to energy loss.

Protons exiting through the *side* patch show exactly the opposite picture. To reach the patch the protons have to cross the magnetic field lines and very few lower energy particles can do that with the help of the random field. In the vicinity of 10^{19} eV the exit spectrum is more than two orders of magnitude short of the injection spectrum. Above 2×10^{20} eV the two exit spectra

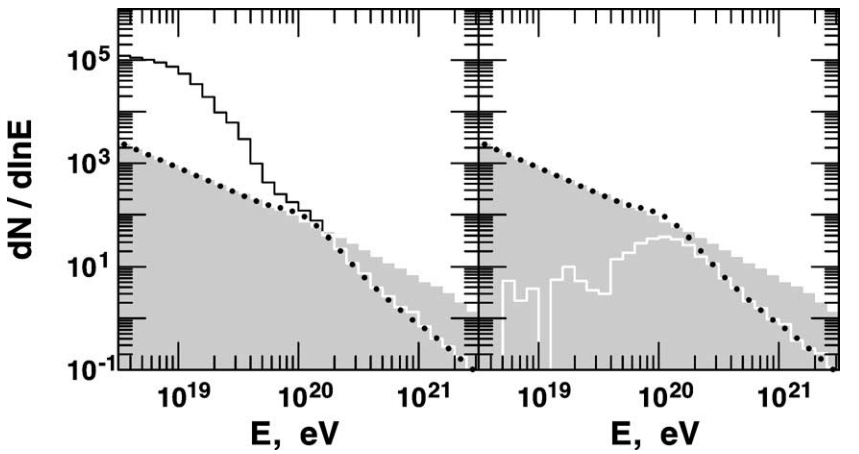

Fig. 5. Energy distribution of protons leaving the *front* patch (left) and the *side* patch (right) at 20 Mpc from an isotropic cosmic ray source. See the text for a description of the geometry. The shaded histogram shows the energy spectra of the protons emitted in the direction of the patches and the dots show the proton energy spectrum at 20 Mpc in the absence of magnetic field.

are identical. If two observers were estimating the proton injection spectra with no account for the magnetic fields at 10^{19} eV, their estimates would differ by four orders of magnitude.

In these simple cases one can scale the effects in proton energy as a function of the magnetic field strength. If $B_{\rm reg}$ were 5 nG, all effects would be the same but at energies that are twice as low. Large scale fields of strength 10 nG extending through a small fraction of the volume of the Universe are not an extreme assumption. The effects demonstrated in Fig. 5 will certainly happen at a certain level in the real Universe.

8. Summary

- All known stable particles that are candidates for the ultra high energy cosmic rays lose energy in interactions with the cosmic microwave background and other astrophysical photon fields.
- The energy losses set a horizon for the sources of such particles (a maximum distance from the observer) and modify the injection spectrum of these cosmic rays.
- Charged UHECR, such as protons and heavier nuclei, scatter in the extragalactic magnetic fields. This scattering causes increased pathlength, decreases the particle horizon, and introduces deflection from the source direction and significant time delay.
- Possibly existing organized extragalactic fields with dimension of 10 Mpc and strength of several nanogauss complicate the propagation patterns and may lead to strong distortions of the particle injection spectrum as a function of the magnetic field, source and observer geometry.
- Only protons of energy well above 10^{20} eV reveal the source spectrum and position after an account for the energy loss on propagation. Hopefully the Auger Observatory, and later EUSO and OWL, will collect significant statistics of such events that will reveal the type and the luminosity of the UHECR sources.

Acknowledgements

Much of the work on which this article is based was performed with R. Engel, D. Seckel and others. This research is supported in part by NASA grant NAG5-10919.

References

[1] J. Linsley, Phys. Rev. Lett. 10 (1963) 146.
[2] K. Greisen, Phys. Rev. Lett 16 (1966) 748.
[3] G.T. Zatsepin, V.A. Kuzmin, Pisma Zh. Exp. Theor. Phys. 4 (1966) 114.
[4] R.J. Protheroe, P.L. Biermann, Astropart. Phys. 7 (1997) 181.

[5] F.W. Stecker, M.H. Salamon, Astrophys. J. 512 (1999) 521.
[6] V.S. Berezinsky, S.I. Grigorieva, Astron. Astrophys. 199 (1988) 1.
[7] C.T. Hill, D.N. Schramm, Phys. Rev. D 31 (1985) 564.
[8] S. Yoshida, M. Teshima, Prog. Theor. Phys. 89 (1993) 833.
[9] F.A. Aharonian, J.W. Cronin, Phys. Rev. D 50 (1994) 1892.
[10] T. Stanev, et al., Phys. Rev. D 62 (2000) 093005.
[11] R.J. Protheroe, P.A. Johnson, Astropart. Phys. 4 (1996) 253.
[12] N. Hayashida, et al., Astropart. Phys. 10 (1999) 303.
[13] T. Stanev, D. Seckel, R. Engel, Phys. Rev. D 68 (2003) 103004.
[14] G. de Vaucouleurs, Second Reference Catalog of Bright Galaxies, University of Texas Press, Austin, 1976.